Tensile Properties of Short Sisal Fiber Reinforced Polystyrene Composites

K. C. MANIKANDAN NAIR,[1] S. M. DIWAN,[2] and SABU THOMAS[1,*]

[1]School of Chemical Sciences, Mahatma Gandhi University, Priyadarshini Hills P.O., Kottayam-686 560, Kerala, India, and [2]Product Application and Research Centre, Reliance Industries Limited, Bombay-400 071, India

SYNOPSIS

The tensile properties of polystyrene reinforced with short sisal fiber and benzoylated sisal fiber were studied. The influence of fiber length, fiber content, fiber orientation, and benzoylation of the fiber on the tensile properties of the composite were evaluated. The benzoylation of the fiber improves the adhesion of the fiber to the polystyrene matrix. The benzoylated fiber was analyzed by IR spectroscopy. Experimental results indicate a better compatibility between benzoylated fiber and polystyrene. The benzoylation of the sisal fiber was found to enhance the tensile properties of the resulting composite. The tensile properties of unidirectionally aligned composites show a gradual increase with fiber content and a leveling off beyond 20% fiber loading. The properties were found to be almost independent of fiber length although the ultimate tensile strength shows marginal improvement at 10 mm fiber length. The thermal properties of the composites were analyzed by differential scanning calorimetry. Scanning electron microscopy was used to investigate the fiber surface, fiber pullout, and fiber–matrix interface. Theoretical models have been used to fit the experimental mechanical data. © 1996 John Wiley & Sons, Inc.

INTRODUCTION

During the past decade there has been a rapid growth in the development and study of composite materials. Natural fibers like jute, silk, sisal, etc. appear to have gained importance as fillers in plastics because of their low cost, low density, flexibility, rough surface, and reduced wear of processing machinery.[1] Moreover they are biodegradable and are obtained from renewable sources. The performance of cellulose fibers as reinforcing filler depends on factors like aspect ratio, orientation of fibers, and fiber–matrix adhesion.[2]

Sisal fiber is a lignocellulosic material extracted from the plant *Agave veracruz* and is available in quantity in the southern parts of India. The incorporation of sisal fiber into plastics and elastomers to obtain cost reduction and reinforcement have been reported by various workers. Paramasivan and Abdulkalam[3] investigated the feasibility of developing polymer-based composites using sisal fiber. Pavithran et al.[4] reported the impact properties of unidirectionally oriented sisal fiber composite. Recently our research group reported on the use of short pineapple[5] and sisal fiber for the reinforcement of natural rubber[6-9] and low-density polyethylene[10-14] and various thermosets.[15] However, no work has been reported on the use of sisal fiber for the reinforcement of polystyrene.

The major drawbacks associated with the use of natural fibers as reinforcement in thermoplastics are the poor wettability and weak interfacial bonding with the polymer due to the inherently poor compatibility and dispersability of the hydrophilic cellulosic fibers with hydrophobic thermoplastics. There are several methods that can be used to overcome the problem of poor compatibility between cellulosic fibers and thermoplastics. The use of coupling agents, pretreatment of fibers, grafting, and coating of fibers with suitable chemicals were reported to improve the interfacial adhesion between cellulosic fibers and thermoplastics. Kokta and coworkers[16-18] studied the use of isocyanate treatment, silane coating, and grafting to improve the

* To whom correspondence should be addressed.

Journal of Applied Polymer Science, Vol. 60, 1483–1497 (1996)
 CCC 0021-8995/96/091483-15

mechanical properties of polystyrene–chemithermomechanical pulp (CTMP) composites. Joseph et al.[19] reported that a considerable improvement in the mechanical properties of polyethylene/sisal fiber composite can be achieved by a pretreatment of the fibers with isocyanate derivatives of cardanol. Acetylation of the sisal fiber to improve the mechanical properties of natural rubber–sisal fiber composite was reported by Varghese et al.[6] In the present work we try to overcome the problem of compatibility by a new approach, i.e., by benzoylating the fiber, which makes the fiber more hydrophobic and compatible with polystyrene.

In this article we report the results of our studies on the tensile properties of short-sisal fiber–reinforced polystyrene composites with special reference to the effect of fiber length, fiber orientation, and fiber loading. The effects of benzoylation to improve the fiber–matrix adhesion and tensile properties of the composite are also reported. Scanning electron microscopy (SEM) studies were carried out to get an insight into fiber–matrix adhesion and fiber pullout. Thermal properties of the composite are characterized by differential scanning calorimetry (DSC). Finally, theoretical models were used to fit the experimental mechanical data.

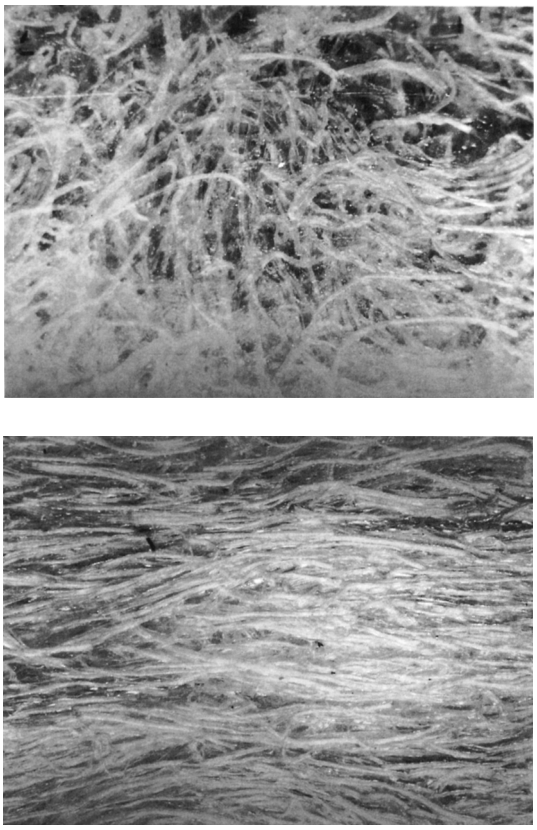

Figure 1 Optical photograph of the surface of (a) randomly oriented fiber composite and (b) unidirectionally oriented fiber composite.

EXPERIMENTAL

Materials

Polystyrene (POLYSTRON 678 SF-1, crystal grade) was supplied by Polychem Limited, India, and the sisal fiber was obtained from local sources. The essential physical properties of these materials are listed in Table I. All the other chemicals used in this work were reagent grade and used without purification.

Preparation of Fiber

Untreated Fiber

The fiber was cleaned and chopped into the desired length ranging from 2 to 10 mm. The chopped fibers were washed with water and dried at 70°C in an oven before making the composites.

Table I Physical Properties of Polystyrene and Sisal Fiber

Physical Property	Polystyrene	Sisal Fiber	Benzoylated Sisal Fiber
MFI (g/10 min)	15	—	—
Density (g/cm^3)	1.05	1.4	1.46
Softening point (°C)	100	—	—
Elongation at break (%)	9	4–9	9–11
Cellulose content (%)	—	85–88	—
Lignin content (%)	—	4–5	—
Tensile strength (MPa)	34.9	450–700	500–650
Young's modulus (MPa)	390	7000–13000	4000–6000

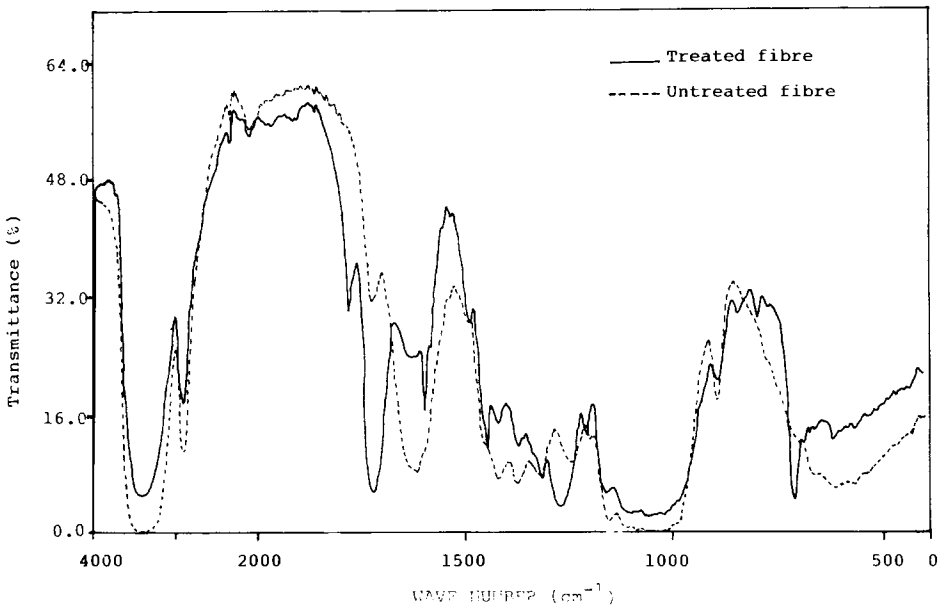

Figure 2 IR spectra of untreated and benzoylated sisal fiber.

Benzoylated Fiber

A fixed amount (35 g) of washed fiber was soaked in 18% NaOH solution for half an hour, filtered, and washed with water. The treated fiber was suspended in 10% NaOH solution and agitated well with 50 mL benzoyl chloride. The mixture was kept for 15 min, filtered, washed thoroughly with water, and dried between filter paper. The isolated fiber was then soaked in ethanol for 1 h to remove the unreacted benzoyl chloride and finally was washed with water and dried.

Preparation of PS–Sisal Fiber Composite

The polystyrene–sisal fiber molding composites were prepared by a solution mixing technique developed by our research group.[19] In this method fiber was mixed with a viscous slurry of polystyrene in toluene that was prepared by adding toluene to a melt of the polymer. The mix was then completely dried to remove the solvent and then was subjected to extrusion through a hand-operated injection molding machine. Composites containing 10, 20, and 30% by weight of untreated fiber and benzoylated fiber were prepared using fibers of length 2, 6, and 10 mm. These composites were denoted by symbols U 106 (L), B 106 (T), U 206 (R), etc. In these notations the first letter denotes the nature of the fiber, viz. "U" for untreated fiber and "B" for benzoylated fiber. The first and second digits together denote the weight percentage of fiber and the third digit denotes the length of the fiber. The letter in parentheses gives the orientation of the fiber in the composite (L, longitudinally oriented; T, transversely oriented; R, randomly oriented).

Preparation of Composite Sheets

Randomly Oriented Fiber Composite

Randomly oriented composite sheet of dimensions 120 × 12.5 × 3 mm were prepared by injection molding of the composite at 150 ± 5°C into a mold of dimensions 120 × 12.5 × 3 mm, using a hand-operated ram-type injection molding machine. Figure 1(a) shows the optical photograph of the surface of a randomly oriented composite.

Oriented Fiber Composite

The specimens of oriented fiber composites were prepared by a combination of injection molding and compression molding. The composite was first processed to get 4-mm-thick cylindrical rods using an injection molding machine. Rectangular specimens measuring 120 × 26.5 × 2.5 mm were prepared by aligning the extrudate (120 mm long and 4 mm diameter) in a leaky mold[20,21] and then compression molding at a pressure of about 8 MPa and a temperature of 150 ± 5°C. The specimens were removed after cooling the mold below 50°C. Figure 1(b) shows the optical photograph of the surface of a unidirectionally oriented composites.

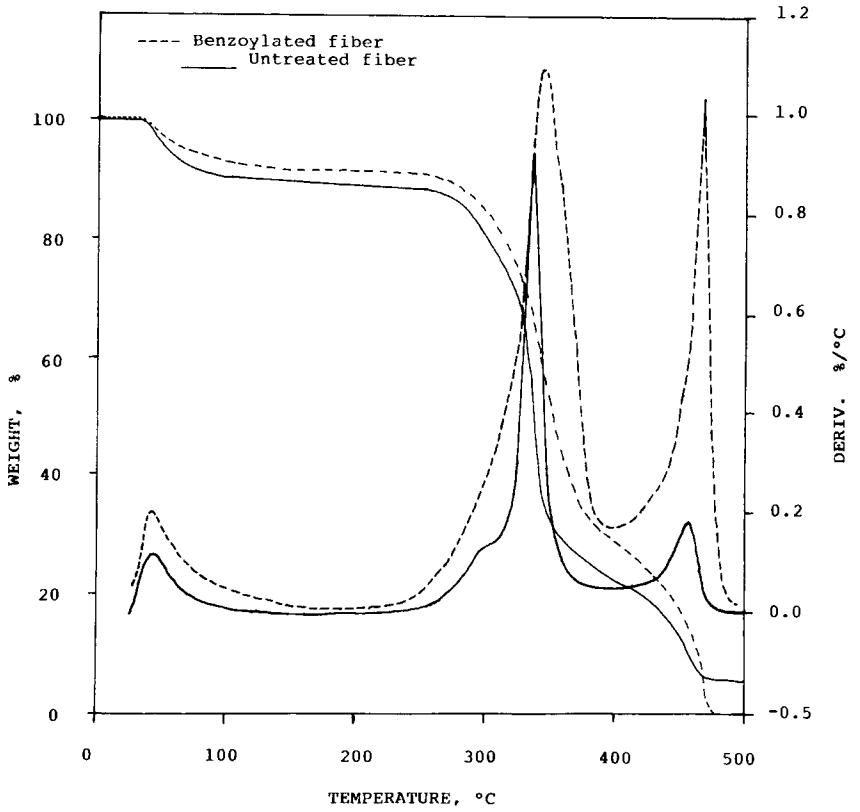

Figure 3 TGA and DTGA curves of untreated and benzoylated sisal fiber.

Mechanical Testing

The tensile properties of the composites were measured on a Good Brand–Jeffreys Testomeric Micro-500 testing machine at a cross head speed of 5 mm min^{-1} and a gauge length of 50 mm. A standard UTM tensile test program was used to evaluate the mechanical properties (ultimate tensile strength, Young's modulus, elongation at the break, and the yield point). The test specimens were rectangular in shape with dimensions 120 × 12.5 × 3 mm for randomly oriented composites and 120 × 26.5 × 2.5 mm for unidirectionally oriented composites. The tensile properties were reported after taking the average value of five measurements.

Thermal Analysis

The thermal behavior of untreated and benzoylated sisal fibers were studied using a Du Pont 2000 TGA system. Differential scanning calorimetry (DSC) experiments were carried out on a Perkin–Elmer DSC system. Each sample undergoes a programmed heating variation in the range of 30–150°C at a rate of 10°C min^{-1}. The glass transition temperature (T_g) has been determined for pure polystyrene and composites containing untreated fiber and benzoylated fiber. T_g is reported as the midpoint of the transition region.

IR Analysis

A Shimadzu IR-490 spectrophotometer was used to analyze the changes in chemical structure of benzoylated fiber. Powdered fiber pelletized with potassium bromide was used for recording the spectra.

SEM Examinations/Optical Microscopy Studies

Surface morphology of untreated fiber, benzoylated fiber, and surfaces of the fractured specimens were examined using a JEOL scanning electron microscope. An optical stereomicroscope was used for observing the fiber orientation.

RESULTS AND DISCUSSION

Synthesis and Characterization of Benzoylated Sisal Fiber

The reaction between the cellulosic —OH group of sisal fiber and benzoyl chloride may be shown as

Table II The Weight Losses of Untreated and Benzoylated Sisal Fiber at Various Temperatures

Sample (wt %)	Sisal Fiber (°C)	
	Untreated	Benzoylated
1	40	40
5	95.6	95.6
10	195	260
15	280	300
20	300	310
25	310	320
30	320	330
40	335	342
50	—	352
60	343	365
70	355	390
80	415	440
90	463	463

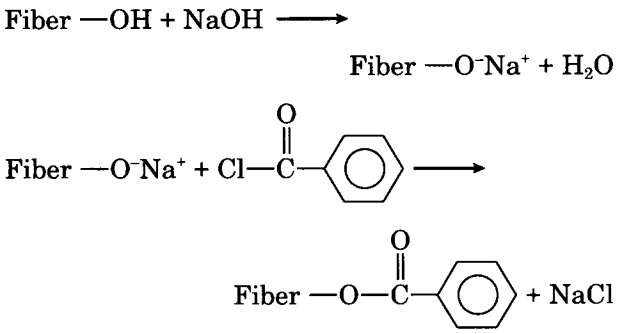

where fiber —OH represents any hydroxyl group in the fiber cellulose components. Because some of the components of the fiber are extractable with sodium hydroxide, it is difficult, if not impossible, to find the extent of reaction. A higher ratio of 1.5 g of benzoyl chloride for 1 g of fiber can be used without considerable deterioration in the physical properties and fibrous nature of the fiber and is the one used in the present work. The oxygen linkage to the fiber is a hydrolyzable bond. However, a more detailed investigation is necessary to understand the susceptibility of the ester group in benzoylated fiber to hydrolysis. Experiments are in progress in this direction.

The chemical structure of benzoylated fiber was remarkably changed as indicated by IR spectra (Fig. 2) of treated and untreated fiber. Hydroxyl vibration absorption at about 3400 cm^{-1} diminished after benzoylation as a result of esterification of the hydroxyl group. Absorption bands around 1950, 1600, and 710 cm^{-1} indicate the presence of aromatic groups, and the peaks around 1725 and 1300 cm^{-1} indicate the presence of ester groups.

Figure 3 shows the TGA and DTGA curves of untreated and benzoylated sisal fiber. The weight losses of untreated and benzoylated sisal fibers at various temperatures are given in Table II. The first peak between 60 and 100°C corresponds to the heat of vaporization of water in the sample. The second peak at about 325°C is due to the thermal depolymerization of hemicellulose and the cleavage of the glucosidic linkages of cellulose.[22] The third peak at about 450°C may be due to the further breakage of the decomposition products of stage II, leading to the formation of tar through levoglucosan.[23] From the data it is clear that benzoylated sisal fiber exhibits a higher thermal stability compared to untreated fiber. This may be attributed to the substitution of bulky phenyl groups in the fiber that restrict the segmental mobility, thereby increasing the stiffness of the cellulose backbone. It is also partially due to the fact that some of the components of the fiber, such as lignocellulose, that degrade at a lower temperature may be extracted during alkali treatment. The improvement in the thermal stability of the fiber will lead to the better service performance of the composites at elevated temperatures.

Figure 4(a,b) show the SEM photographs of untreated sisal fiber, and the treated surfaces are shown in Figure 4(c,d). These figures indicate a reduction in the thickness of the fiber upon benzoylation. This may be due to the leach out of alkali-soluble fractions like waxy layer, lignin, etc. during alkali treatment and benzoylation. Moreover the treatment produces a number of small voids on the surface of the fiber that promote mechanical interlocking between the fiber and the matrix. SEM photographs also show a rough surface for the treated fiber. Table I gives the physical properties of benzoylated sisal fiber. The results indicate a considerable deterioration in modulus as a result of benzoylation. This may be due to the presence of voids as a result of the leaching out of fiber components caused by the benzoylation process. The values of ultimate tensile strength and elongation at break, however, remain almost same as those of untreated fiber.

Fiber Length Distribution

The distribution of fiber lengths can be represented in terms of moments of the distribution in the way a polymer chemist describes molecular weight distribution.[24,25] The number and weight average lengths can be defined as

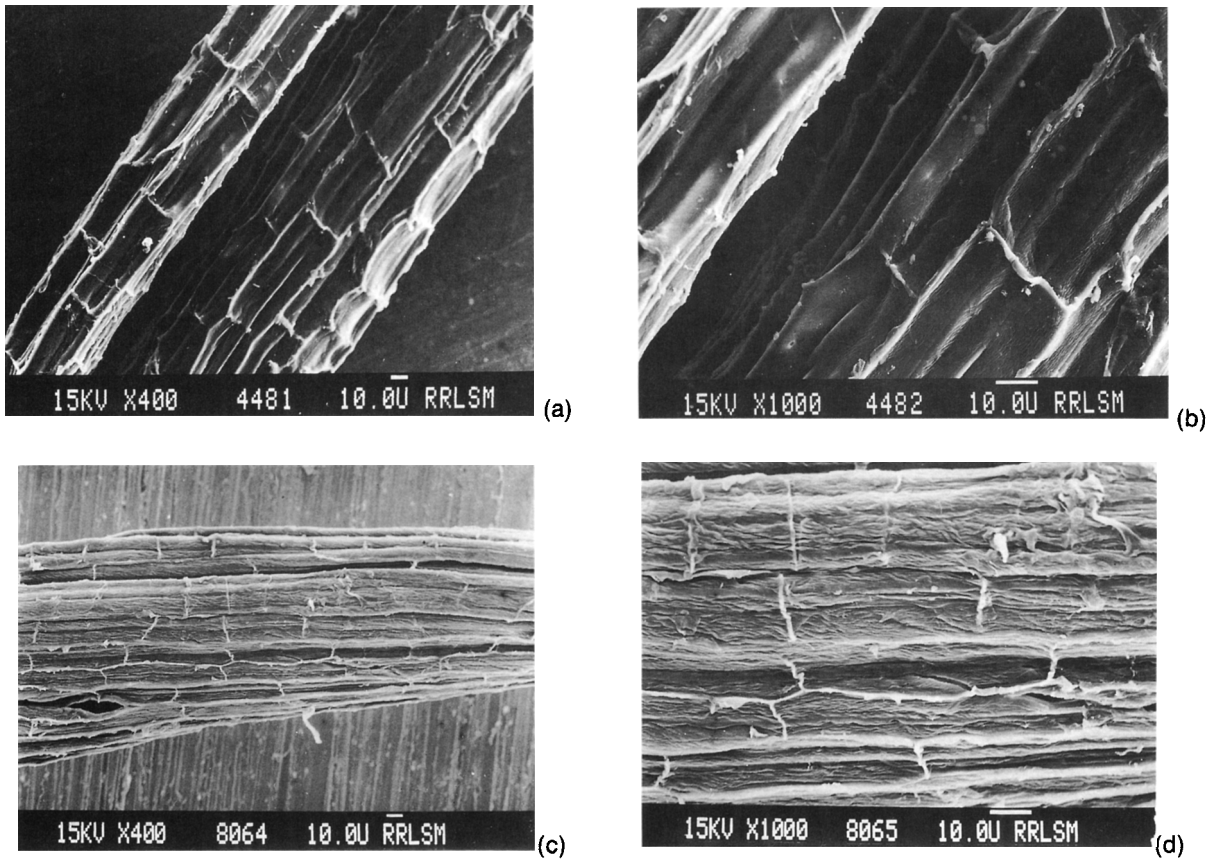

Figure 4 SEM photograph of the surface of (a) untreated sisal fiber, (b) untreated sisal fiber (magnified view), (c) benzoylated sisal fiber, and (d) benzoylated sisal fiber (magnified view).

$$\bar{L}_n = \frac{N_i L_i}{N_i} \quad (1)$$

and

$$\bar{L}_w = \frac{N_i L_i^2}{N_i L_i} \quad (2)$$

where $\bar{L}_n$ is the number average fiber length; $\bar{L}_w$ is the weight average fiber length; and N_i is the number of fibers having length L_i.

Table III Fiber Length Distribution Index

Sample	$\bar{L}_n$ (mm)	$\bar{L}_w$ (mm)	L_w/L_n
Sisal fiber			
Chopped	6.016	6.121	1.017
Extracted from composite	5.687	5.746	1.010

The value of $\bar{L}_w/\bar{L}_n$, the polydispersity index, can be taken as a measure of fiber length distribution. As the fiber length distribution becomes broader, the value $\bar{L}_w/\bar{L}_n$ should increase. Table III summarizes the values of $\bar{L}_n$, $\bar{L}_w$ and $\bar{L}_w/\bar{L}_n$ based on 100 fibers for the chopped sisal fiber and fiber extracted from the composite. The low values of $\bar{L}_w/\bar{L}_n$ indicate

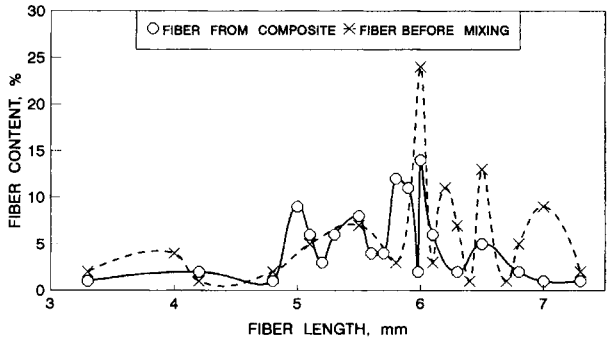

Figure 5 Fiber distribution curves of chopped sisal fiber and fiber extracted from composite.

Table IV Tensile Properties of Polystyrene–Untreated Sisal Fiber Composite as a Function of Fiber Length

Fiber Length (mm)	Ultimate Tensile Strength (MPa)	Young's Modulus (MPa)	Elongation at Break (%)
2	21.12	666	6
6	21.3	629.6	9
10	25.06	657.1	9

Longitudinally oriented 10% fiber composite.

a narrow fiber length distribution before and after mixing. The fiber distribution curve (Fig. 5), however, indicates a slight shift to the lower aspect ratio after mixing.

Mechanical Properties

Effect of Fiber Length

In the case of fiber-reinforced composites there exist a critical aspect ratio at which the mechanical properties of the composites are maximized. The critical aspect ratio depends on the volume fraction of the fiber and also on the ratio of the modulus of fiber to the matrix modulus.[26] At low fiber volume fraction the fibers play no major role, and the strength of the composite is matrix dominated. The strength of the composite was found to increase above a critical volume fraction of the fiber, which in fact depends on the aspect ratio. The critical volume fraction was found to decrease with increase in aspect ratio. At relatively low fiber content, the critical aspect ratio remains almost constant, which, however, shows a sharp decrease at higher volume fraction.[27] As the fiber length increases there is a chance for better orientation, which may lead to an improvement in mechanical properties of the composite. In our earlier studies, we reported that in the case of a low density polyethylene/sisal system[10] the critical fiber length was 6 mm. For natural rubber/sisal[6] and natural rubber/coir fiber system[28] the critical fiber length was found to be 10 mm.

To study the effect of fiber length on the tensile properties of the present system, 10% fiber containing composites with average fiber length of 2, 6, and 10 mm were prepared. Fiber content was limited to 10% because injection of the composite was found difficult at higher fiber loading for 10-mm composite. The mechanical properties of the composites (Table IV) show no considerable variation with change in fiber length, although ultimate tensile strength shows marginal increase at 10-mm fiber length. However, to overcome the difficulty in processing, fibers having 6 mm length was used for further studies.

Effect of Fiber Loading and Orientation

The tensile properties of highly viscous thermoplastics or rubber materials are governed by several factors, such as dispersion problems (agglomerate formation), increase of stress concentration points at fiber ends, and entrapped air during mixing (wetting problems).[29] In the case of polystyrene specimens Murray and Hull[30,31] observed that microvoids and cavities occurred within the crazes at the fiber ends and coalesced to generate planner cavities and or cracking within the crazes. The chances for some amount of opened cleavage-type fracture during the pull out process of fibers were also reported.[32] The broken ends of fibers formed during the tensile deformation may induce crazes and cracks in the matrix and may lead to a decrease in the tensile strength.[28] This phenomenon is more pronounced in samples where the chances of breaking of fibers are higher.

Table V Variation of Tensile Properties of PS–Untreated Sisal Fiber Composite as a Function of Fiber Loading and Fiber Orientation

Fiber Loading (wt %)	Ultimate Tensile Strength (MPa)			Young's Modulus (MPa)			Elongation at Break (%)		
	L	T	R	L	T	R	L	T	R
0	34.90	34.90	34.90	390	390	390	9	9	9
10	21.30	14.75	18.16	629	596.8	516.83	9	5	7
20	43.20	12.37	25.98	999.9	487.9	553.7	8	3	6
30	45.06	11.04	20.42	998	577.6	624.3	7	2	4

Fiber length was 6 mm. L, longitudinal; T, transverse; R, randomly oriented.

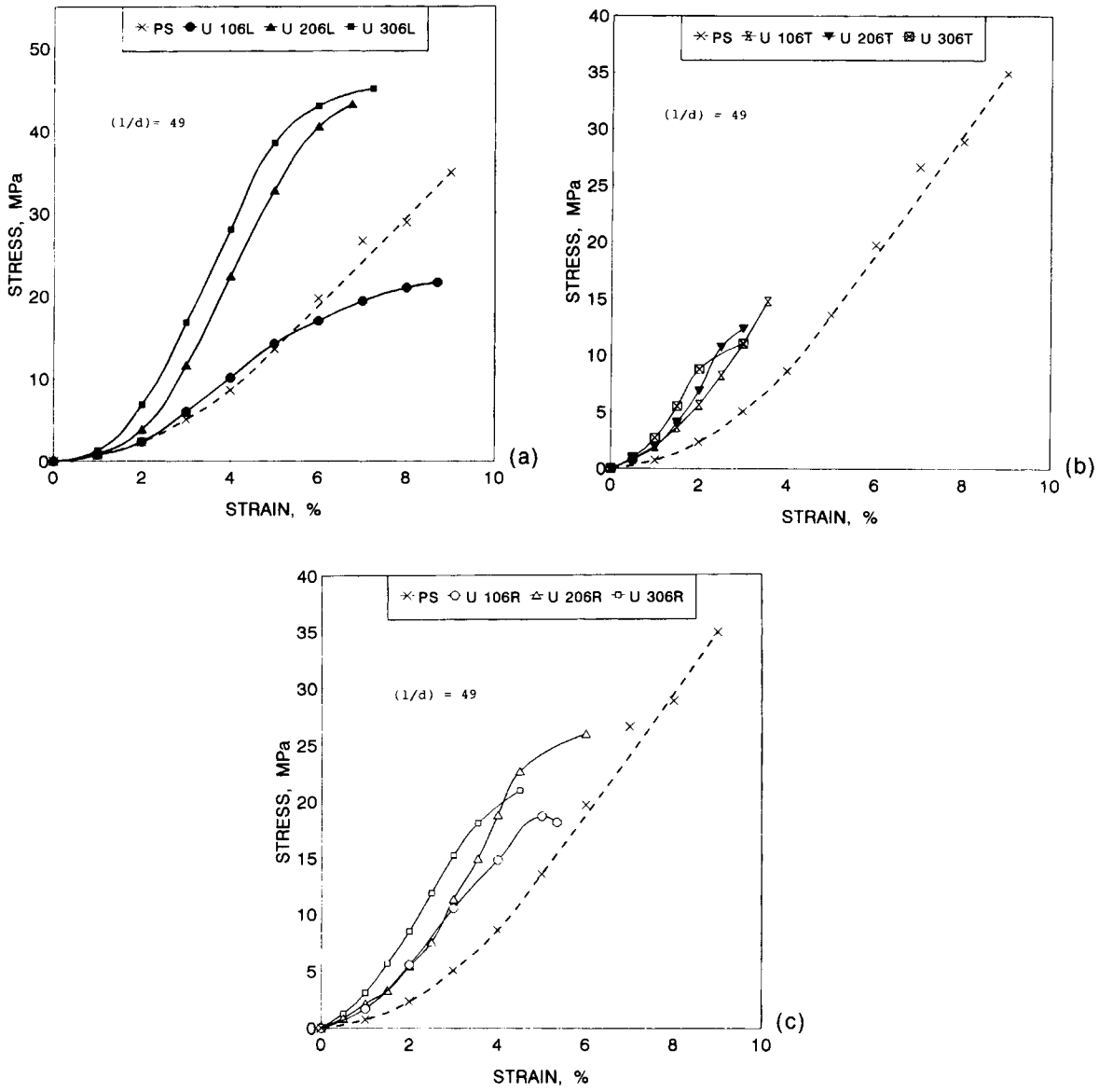

Figure 6 Stress–strain curves of pure polystyrene and untreated sisal fiber reinforced polystyrene containing (a) longitudinally oriented fiber, (b) transversely oriented fiber, and (c) randomly oriented fiber.

The effect of fiber loading and orientation of the fiber on the tensile properties of polystyrene–sisal fiber composite can be readily seen from the data given in Table V and Figures 6–9. In the case of longitudinally oriented fiber composite, it is found that initially there is a reduction in ultimate tensile strength at 10% fiber loading [Figs. 6(a) and 8]. However, increase in fiber loading to 20% improves the tensile strength considerably and produces no appreciable change with further increase of loading. At 10% fiber loading the fiber may act as a flaw in the matrix, reducing the tensile strength of the composite. At low fiber loading the matrix is not restrained by enough fibers and highly localized strain occurs in the matrix at low stresses, causing the bond between matrix and fiber to break, leaving the matrix diluted by nonreinforcing debonded fibers. As the fiber concentration increases, the stress is more evenly distributed and the strength of the composite increases. The modulus values of longitudinally oriented fiber composites increase with fiber content up to 20% loading and level off with further loading. In this case because the fibers are oriented perpendicularly to the direction of the crack

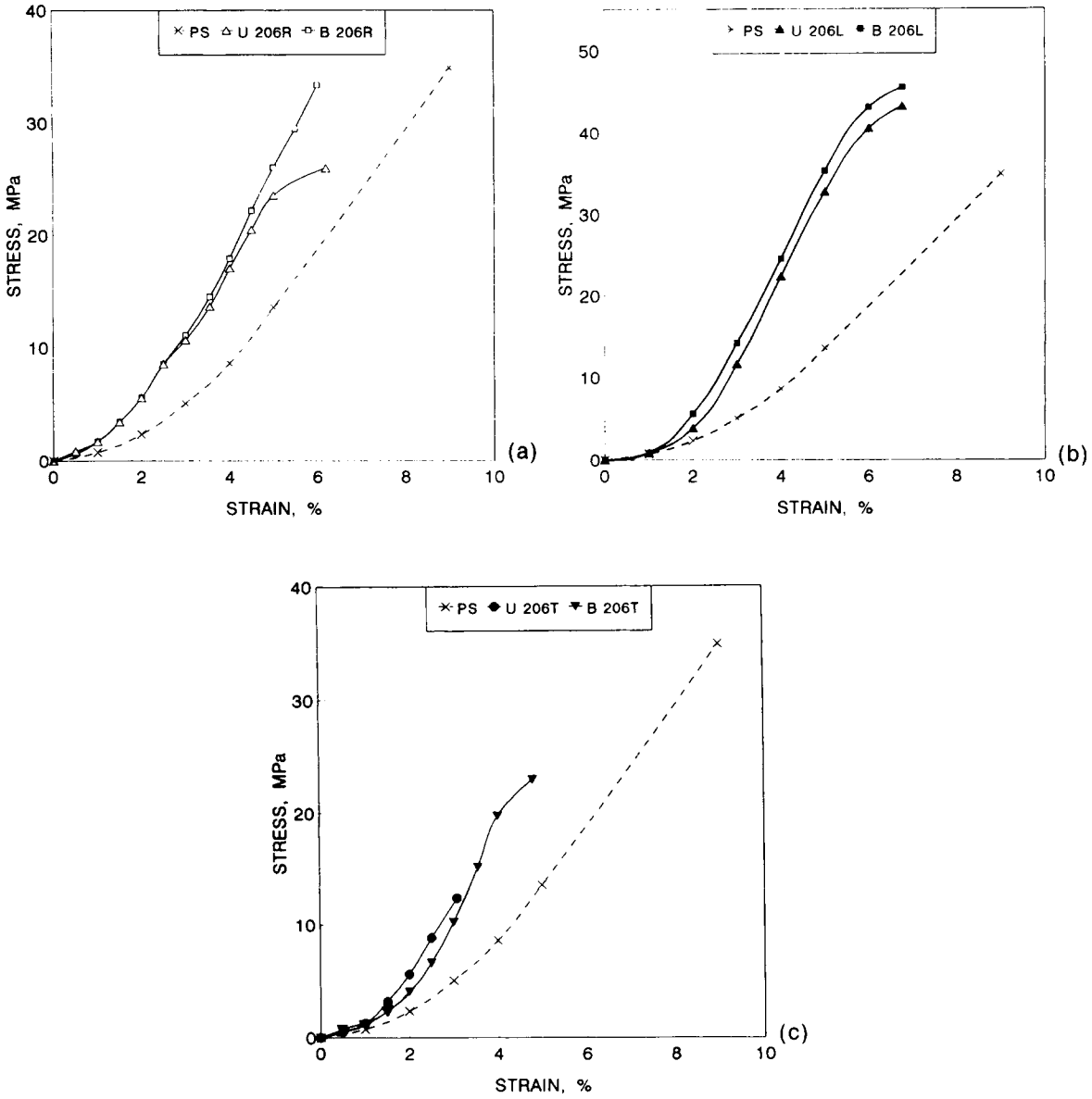

Figure 7 Stress–strain curve of 20% untreated and benzoylated sisal fiber-reinforced polystyrene composite with fibers (a) randomly oriented, (b) longitudinally oriented, and (c) transversely oriented.

propagation, the crack will be hindered. This accounts for the increase in tensile strength and modulus.

The stress–strain curves of transversely oriented fiber composite [Fig. 6(b)] show a considerable deterioration in strength and strain with increase in fiber loading. In this case the crack propagates in the direction of fiber alignment. The transversely oriented fibers act as barriers and prevent the distribution of stresses throughout the matrix, and this in turn causes higher concentration of localized stresses. This explains the reduction in the tensile properties of transversely oriented composite. In this case the modulus shows a value that is higher than that of polystyrene and lower than those of longitudinally oriented composite.

Figure 6(c) shows the stress–strain behavior of randomly oriented fiber composite. These composites show tensile strength and strain that lies in between those of longitudinally and transversely oriented fiber composites as expected. At 20 and 30% fiber loading the modulus values also show a similar trend. At 10% fiber loading the modulus shows a value less than that of transversely and longitudi-

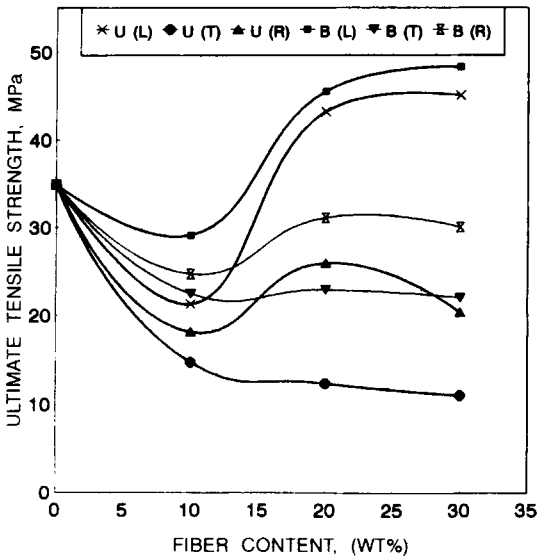

Figure 8 Variation of the tensile strength of untreated and benzoylated sisal fiber composite as a function of fiber content.

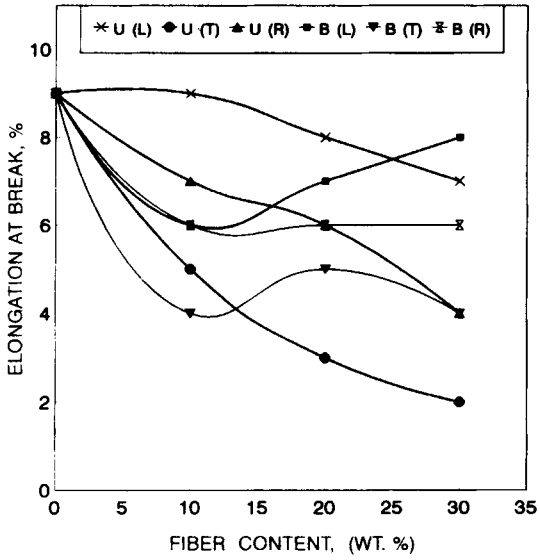

Figure 9 Variation of elongation at break values of untreated and benzoylated sisal fiber composite as a function of fiber content.

nally oriented fiber composite. The reason for this reduction in modulus is not clear. We have observed this anomaly only at 10% fiber loading. Experiments are in progress to understand this abnormal behavior.

The data given in Table V and Figure 9 also show that in almost all experiments the ultimate elongation of composites is less than that of unfilled polymer and decrease with increasing fiber concentration. Stress–strain curves [Fig. 6(a–c)] show a brittle-type failure for both unfilled and reinforced specimens.

Effect of Chemical Treatment

Figure 7(a–c) show the stress–strain behavior of 20% untreated and benzoylated fiber-reinforced polystyrene composites in which the fibers were oriented in randomly, longitudinally, and transverse directions, respectively. The stress–strain curves of both untreated and benzoylated fiber-reinforced composite show a similar trend. However, the strength of treated composite shows higher values than those of untreated composite. As expected, randomly oriented treated fiber composite [Fig. 7(a)] shows lower modulus value compared to untreated composite. However longitudinally oriented [Fig. 7(b)] and transversely oriented [Fig. 7(c)] treated fiber composites show modulus values higher than that of untreated composites. In the case of longitudinally and randomly oriented composites the treatment produces no considerable

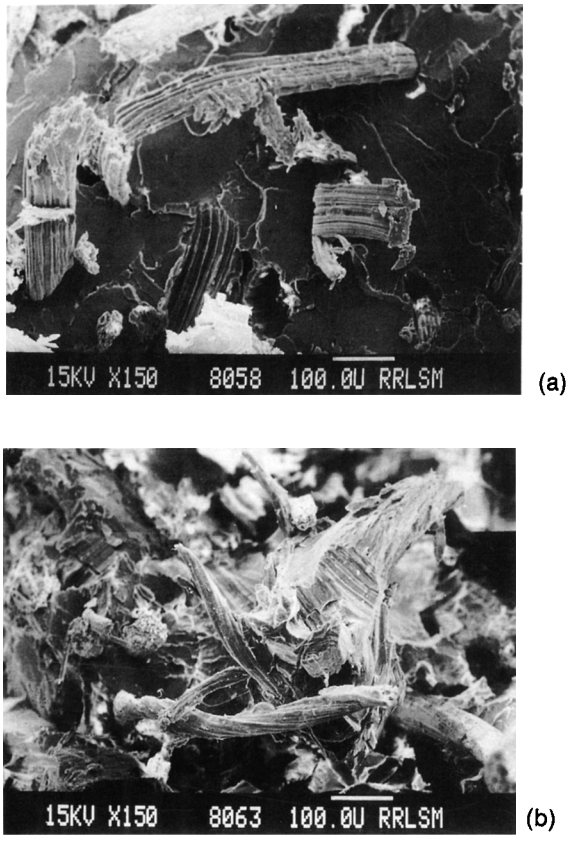

Figure 10 (a) SEM photograph of the fractured surface of untreated sisal fiber reinforced polystyrene composite showing fiber pullout. (b) SEM photograph of the fractured surface of benzoylated sisal fiber reinforced polystyrene composite showing fiber breakage.

Table VI Tensile Properties of Polystyrene–Benzoylated Sisal Fiber Composite as a Function of Fiber Loading and Orientation

Fiber Content (wt %)	Ultimate Tensile Strength (MPa)			Young's Modulus (MPa)			Elongation at Break (%)		
	L	T	R	L	T	R	L	T	R
0	34.9	34.9	34.9	390	390	390	9	9	9
10	29.14	22.49	24.72	800	660	457.4	6	4	6
	(21.30)	(14.75)	(18.16)	(629)	(596.8)	(516.83)	(9)	(5)	(7)
20	45.52	22.96	31.14	1026	664.7	543.3	7	5	6
	(43.20)	(12.37)	(25.98)	(999.9)	(487.9)	(553.7)	(8)	(3)	(6)
30	48.3	22.08	30.09	1125	701.3	710.7	8	4	6
	(45.06)	(11.04)	(20.42)	(998)	(577.6)	(624.3)	(7)	(2)	(4)

Fiber length was 6 mm. The values in parantheses give the properties of untreated fiber composites.

variation in strain. However, transversely oriented composite shows considerable increase in strain as a result of treatment.

The influence of benzoylation of the fiber on the tensile properties of the composites appears in Table VI and Figure 8. To compare the tensile properties of untreated and benzoylated fiber composites, the improvement in tensile properties are listed in Table VII.he values show considerable improvement in tensile properties as a result of benzoylation. The elongation at break value, however, remains almost same for both benzoylated and untreated fiber composites (Fig. 9). The improvement in tensile strength and modulus are attributed to the better adhesion between the treated fiber and polystyrene. This can be readily understood from the SEM photographs of the fractured surface of untreated sisal fiber composite and benzoylated fiber composite [Fig. 10(a) and (b)]. The fracture surface of untreated fiber composite shows [Fig. 10(a)] holes and fiber ends indicating that most of the fibers have come out without breaking during the fracture of untreated composite. This suggests poor adhesion between the matrix and fiber. The fracture surface of treated fiber composite [Fig. 10(b)] shows fiber breakage rather than pullout, which in turn indicates better interfacial strength. This is again clear from the SEM photographs of the surfaces of treated and untreated fiber stripped out from the composite [Fig. 11(a), (b), and (c)]. The surface of the treated fiber was found to have a coating of polystyrene, suggesting better interfacial interaction [Fig. 11(b) and (c)]. Figure 11(d) (untreated) and (e) (treated) also support this view.

Also, in the case of treated fiber composite, the effect of fiber loading and fiber orientation on the tensile properties follow a trend similar to untreated composites (Table VI).

As explained earlier, benzoylated fiber composite shows considerable improvement in tensile strength, and percentage of improvement is in the order, transversely oriented > randomly oriented > longitudinally oriented fiber composite (Table VII). This can be explained as follows. As the orientation goes from longitudinal to transverse, the failure mode changes from fiber failure to interface shear and then to transverse matrix failure. In the case of transversely oriented specimen the interface becomes more exposed, and hence an improvement in interface strength due to benzoylation of the fiber leads to considerable enhancement in the strength of the transversely oriented composite. In the case of randomly oriented composite the interface is exposed to an extent that is in between the longitudinally oriented and transversely oriented composite. This in fact accounts for the improvement in tensile strength of transversely and randomly oriented composites compared to longitudinally oriented composites.

Table VII Percentage Improvement of Tensile Properties of Polystyrene–Sisal Fiber Composite as a Result of Benzoylation of the Fiber at Different Fiber Loading and Orientation

Fiber Loading (wt %)	Ultimate Tensile Strength (MPa)			Young's Modulus (MPa)		
	L	T	R	L	T	R
10	38	52	36	27	11	−11
20	5	85	20	3	36	−2
30	7	100	47	13	21	14

Average fiber length was 6 mm.

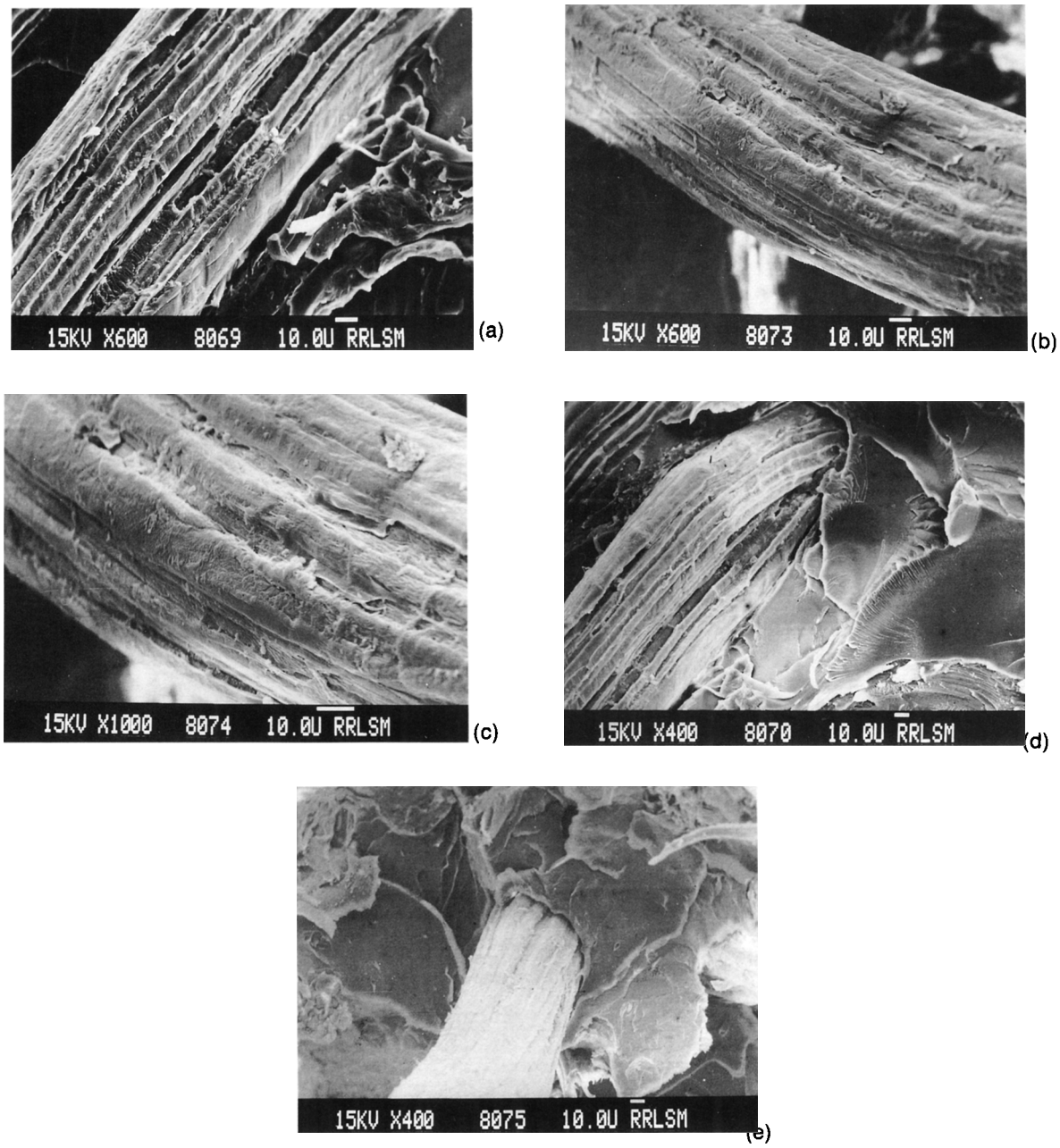

Figure 11 SEM photograph of the surface of (a) untreated sisal fiber stripped out from the composite, (b) benzoylated sisal fiber stripped out from the composite, and (c) benzoylated sisal fiber stripped out from the composite (magnified view). SEM photograph of (d) an untreated sisal fiber protruded from the polystyrene matrix, and (e) a benzoylated sisal fiber protruded from the polystyrene matrix.

Because the benzoylation reduces the modulus of the sisal fiber considerably, the modulus of the benzoylated fiber composites were expected to be lower than that of untreated fiber composites. However, the experimental values (Table VI) show a considerable improvement in modulus in the case of longitudinally and transversely oriented treated fiber composites. At 30% loading the randomly oriented treated fiber composites also show an improvement in modulus. This improvement in modulus may be attributed to the better adhesion between the benzoylated fiber and polystyrene matrix. The fiber–

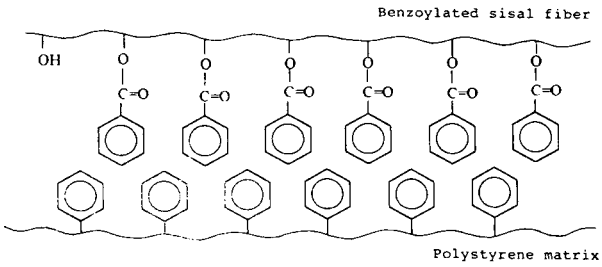

Figure 12 A hypothetical model of the interface of benzoylated sisal fiber reinforced–polystyrene composite.

matrix adhesion in this case is considerably strong and overshadows the effect of decrease in modulus of the fiber upon benzoylation. Similar results on the improvement of modulus of the composites upon treatment has been reported by several workers.[19,33,34]

The improvement in the tensile properties of treated fiber composite is attributed to the presence of phenyl-structure in treated fiber similar to that of polystyrene, which improves the thermodynamic compatibility between benzoylated fiber and polystyrene. As explained earlier, another contributing factor to the improved properties is the reduction in the hydrophilicity of fiber as a result of benzoylation, which makes the fiber more compatible with hydrophobic polystyrene. A hypothetical model of the polystyrene–benzoylated fiber interface is shown in Figure 12.

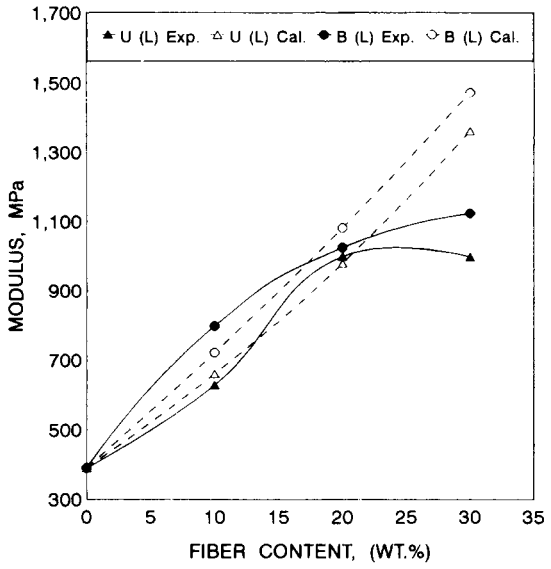

Figure 14 Comparison of the experimental moduli and theoretical moduli of polystyrene–sisal fiber composite.

DSC Analysis

The changes of the glass transition temperature of the polymers due to the incorporation of fibers and

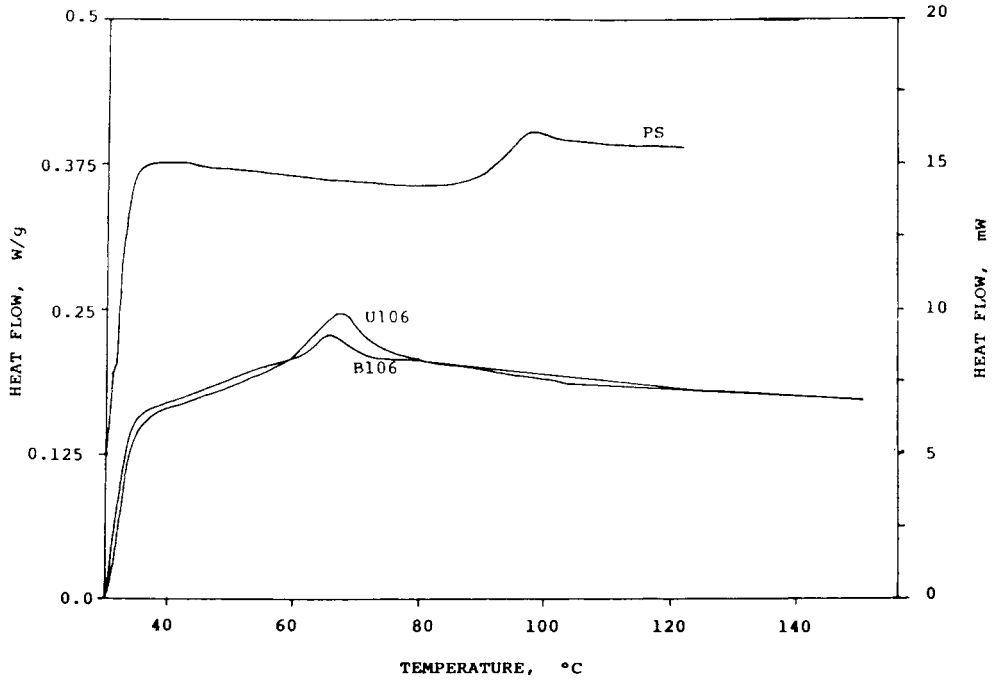

Figure 13 DSC curves of polystyrene, untreated sisal fiber–polystyrene composite and benzoylated sisal fiber–polystyrene composite.

whiskers were reported by various workers. Rebenfeld et al.[35] reported that the T_g of neat polyphenylene sulfide was depressed by about 3–5°C by the addition of aramid, glass, and carbon fibers. The addition of benzylated wood in polystyrene lowered the T_g of polystyrene and shifted further to the lower temperatures when the amount of benzylated wood was increased.[36] The lowering of T_g may be attributed to the plasticization effect of the fiber that diffuses or dissolves into the polymer. Figure 13 shows the DSC curves of pure polystyrene, untreated sisal fiber–polystyrene composite and benzoylated sisal fiber composite. The glass transition temperature of pure polystyrene was found to be 93°C. The incorporation of 10% untreated sisal fiber and benzoylated sisal fiber reduces the T_g of polystyrene to 63 and 61°C, respectively. The extent of decrease in T_g is more pronounced in the case of benzoylated fiber composite, and this may be attributed to the improved plasticization effect of benzoylated fiber.

Theoretical Modeling

In the literature, a number of theories and equations have been developed to predict the mechanical properties of the composites. The modulus of a uniaxially oriented composites is given by the Halpin–Tsai equations.[37,38] According to this equation

$$\frac{P}{P_m} = \frac{1 + \xi\eta V_f}{1 - \eta V_f} \tag{4}$$

where

$$\eta = \frac{P_f/P_m - 1}{P_f/P_m + \xi} \tag{5}$$

Here, P is the composite modulus; P_f is the modulus of the fiber; P_m is the matrix modulus; ξ is the empirical factor, which is a measure of the reinforcement, which depends on fiber geometry, fiber distribution, and loading conditions; and V_f is the volume fraction of the fiber.

Figure 14 compares the theoretical and experimental moduli of longitudinally oriented untreated and benzoylated sisal fiber–polystyrene composites. For a value of $\xi = 12$ for untreated sisal fiber and $\xi = 88$ for benzoylated fiber, the figure shows good agreement between the experimental and theoretical values up to 20% fiber loading. However, when the fiber loading is more than 20% the experimental modulus values deviate from theory. This may be attributed to the poor orientation of the fiber in the composite at higher fiber loading.

CONCLUSIONS

The following conclusions can be made from this study.

1. Variation in fiber length produces no considerable change in the modulus of polystyrene–sisal fiber composite. However, the composite exhibited maximum tensile strength at a fiber length of about 10 mm (aspect ratio = 82).
2. There is an initial reduction in tensile strength of polystyrene at 10% fiber loading. Increase of fiber loading to 20% improves the tensile strength considerably and produces no appreciable change with further loading.
3. The incorporation of sisal fiber considerably improves the modulus of the composite.
4. The tensile strength and modulus of the composite was found to follow the order, longitudinally oriented fiber composite > randomly oriented fiber composite > transversely oriented fiber composite.
5. Benzoylation of the sisal fiber considerably improves the tensile properties of the composite.
6. SEM studies show that the interfacial adhesion between the benzoylated fibers and polystyrene matrix are considerably higher compared to that of untreated sisal fiber–polystyrene composite. The incorporation of sisal fiber considerably reduced the glass transition temperature (T_g) of polystyrene. The lowering of T_g is more pronounced in the case of benzoylated fiber.
7. The Halpin–Tsai equation has been used to predict the modulus of the unidirectionally oriented, untreated, and benzoylated fiber composites and the predicted values shows good agreement with the experimental values up to 20% fiber loading. However, at higher fiber loading the predicted values show deviation from the experimental values.

The authors express their appreciation to Dr. Kuruvilla Joseph for the fruitful discussions and Mr. C. Sreekumaran Nair, VSSC, Thiruvananthapuram, for his help in obtaining TGA and DTGA data. We are also grateful to Mr. Peter Koshy, Head Electron Microscopy Instrumentation, RRL, Thiruvananthapuram, for his help in obtaining SEM photographs. Finally the authors thank the referee for the valuable comments.

REFERENCES

1. B. V. Kokta, C. Daneault, and A. D. Beshay, *Polymer Comp.*, **7**, 33 (1985).
2. W. D. Callister, Jr., *Materials Science and Engineering*, John Wiley and Sons, Inc., New York, 1985.
3. T. Paramasivan and A. P. J. Abdulkalam, *Fiber Sci. Tech.*, **7**, 85 (1974).
4. C. Pavithran, P. S. Mukherjee, M. Brahmakumar, and A. D. Damodaran, *J. Mater. Sci. Lett.*, **7**, 882 (1987).
5. J. George, K. Joseph, S. S. Bhagawan, and S. Thomas, *Mater. Lett.*, **18**, 163 (1993).
6. S. Varghese, B. Kuriakose, S. Thomas, and A. T. Koshy, *Indian J. Nat. Rubber Res.*, **5**(1 & 2), 18 (1992); **4**, 55 (1991).
7. S. Varghese, B. Kuriakose, and S. Thomas, *J. Appl. Polym. Sci.*, **53**, 1051 (1994).
8. S. Varghese, B. Kuriakose, S. Thomas, and A. T. Koshy, *J. Adhesion Sci. Technol.*, **8**(3), 235 (1994).
9. S. Varghese, B. Kuriakose, and S. Thomas, *Plast. Rubb. Comp. Proc. Appl.*, **20**, 930 (1993).
10. K. Joseph, S. Thomas, C. Pavithran, and M. Brahma Kumar, *J. Appl. Polym. Sci.*, **47**, 1731 (1993).
11. K. Joseph, C. Pavithran, and S. Thomas, *J. Reinf. Plast. Comp.*, **12**, 139 (1992).
12. K. Joseph, C. Pavithran, and S. Thomas, *Mater. Lett.*, **15**, 224 (1992).
13. K. Joseph, C. Pavithran, and S. Thomas, *Eur. Polym. J.*, to appear.
14. K. Joseph, S. Thomas, and C. Pavithran, *Polymer*, communicated.
15. K. Joseph, S. Thomas, and C. Pavithran, *Eur. Polym. J.*, communicated.
16. D. Maldas, B. V. Kokta, R. G. Raj, and C. Daneault, *Polymer*, **29**, 1255 (1988).
17. D. Maldas, B. V. Kokta, R. G. Raj, and S. T. Sean, *Mater. Sci. Eng.*, **A104**, 235 (1988).
18. H. Datvag, C. Kalson, and H. E. Strom Vall, *Int. J. Polym. Mater.*, **11**, 9 (1985).
19. K. Joseph, S. Thomas, and C. Pavithran, *Compos. Sci. Technol.*, **53**, 99 (1995).
20. C. Pavithran, P. S. Mukherjee, M. Brahmakumar, and A. D. Damodaran, *J. Mater. Sci., Lett.*, **7**, 825 (1988).
21. N. H. Ladizesky and I. M. Ward, *Comp. Sci. Technol.*, **26**, 129 (1986).
22. T. Naugen, E. Zavarin, and E. M. Barall, *J. Macromol. Sci. Rev. Macromol. Chem.*, **20** (1981).
23. M. M. Tang and R. Bacon, *Carbon*, **2**, 211 (1964).
24. H. Morawetz, *Macromolecules in Solution*, 2nd ed., Interscience, New York, 1975.
25. Lech Czarnecki and James L. White, *J. Appl. Polym. Sci.*, **25**, 1217 (1980).
26. Y. Termonia, *J. Mater. Sci.*, **22**, 504 (1987).
27. Y. Termonia, *J. Mater. Sci.*, **25**, 4644 (1990).
28. V. G. Geethamma, R. Joseph, and S. Thomas, *J. Appl. Polym. Sci.*, **55**, 583 (1995).
29. Qi Wang, A. Ait-Kadi, and S. Kaliaguine, *Polymer Comp.*, **13**, 414 (1992).
30. J. Murray and D. Hull, *Polymer*, **10**, 451 (1969).
31. D. Hull, in *Polymeric Materials*, E. Baer, Ed., ASM, Ohio, 1975, pp. 487–550.
32. N. S. Choi and K. Takahashi, *Colloid Polym. Sci.*, **270**, 659 (1992).
33. Qi Wang, S. Kaliguine, and Ait-Kadi, *J. Appl. Polym. Sci.*, **44**, 1107 (1992).
34. Qi Wang, A. Ait-Kadi, and S. Kaliaguine, *J. Appl. Polym. Sci.*, **45**, 1023 (1992).
35. Ludwig Rebenfeld, Glenn P. Desio, and Jame C. Wu, *J. Appl. Polym. Sci.*, **402**, 801 (1991).
36. David N.-S. Hon, and Wayne Y. Chao, *J. Appl. Polym. Sci.*, **50**, 7 (1993).
37. J. C. Halpin and J. L. Kardos, *Polym. Eng. Sci.*, **16**, 344 (1976).
38. E. Baer and A. Moet (Eds.), *High Performance Polymers*, Hanser, New York, 1991, p. 206.

Received December 16, 1994
Accepted November 19, 1995